

# Retention and Transport of Silver Nanoparticles in a Ceramic Porous Medium Used for Point-of-Use Water Treatment

Dianjun Ren and James A. Smith\*

Department of Civil and Environmental Engineering, University of Virginia, Charlottesville, Virginia 22904, United States

**S** Supporting Information

**ABSTRACT:** The retention and transport of silver nanoparticles (Ag-NPs) through a ceramic porous medium used for point-of-use drinking water purification is investigated. Two general types of experiments were performed: (i) pulse injections of suspensions of Ag-NPs in aqueous  $MgSO_4$  solutions were applied to the ceramic medium, and effluent silver was quantified over time; (ii) Ag-NPs were applied directly to the porous medium during fabrication using a paint-on, dipping, or fire-in method, a synthetic, moderately hard water sample with monovalent and divalent inorganic ions was applied to the ceramic medium, and effluent silver was quantified over time. These latter experiments were performed to approximate real-world use of the filter medium. For experiments with Ag-NPs suspended in the inflow solution, the percentage of applied Ag-NPs retained in the ceramic porous medium ranged from about 13 to 100%. Ag-NP mobility decreased with increasing ionic strength for all cases and to a lesser extent with increasing nanoparticle diameter. Citrate-capped particles were slightly less mobile than proteinate-capped particles. For ceramic disks fabricated with Ag-NPs by the paint-on and dipping methods (where the Ag-NPs are applied to the disks after firing), significant release of nanoparticles into the filter disk effluent was observed relative to the fire-in method (where the nanoparticles are combined with the clay, water, grog, and flour before firing). These results suggest that the fire-in method may be a new and significant improvement to ceramic filter design.



## INTRODUCTION

In a recent meta-analysis of water-quality interventions aimed at reducing diarrheal disease in the developing world, Clasen et al.<sup>1</sup> report that point-of-use (e.g., household-level) water-treatment interventions are more effective in improving water quality than interventions at the source. Household water treatment can be more cost-effective over time compared with centralized water treatment and distribution systems.<sup>2</sup>

One of the most promising point-of-use (POU) water-treatment technologies is ceramic water filters manufactured with local labor using clay, water, and a combustible organic material (such as sawdust, flour, or rice husks).<sup>3–5</sup> The clay, combustible material, and water are combined in appropriate proportions and pressed into the shape of a pot and fired in a kiln. During firing, the clay hardens into a ceramic and the sawdust, flour, or rice husk combusts leaving internal porosity for water flow. The pot-shaped filter is placed in a larger, plastic container with a spigot, providing a safe-storage reservoir. An aqueous colloidal suspension of silver nanoparticles (Ag-NPs) is typically applied to the filter after firing using a paint brush or submerging the filter in the aqueous Ag-NP suspension. Presumably, the Ag-NPs lodge in the pores of the ceramic media and provide disinfection action by the gradual release of ionic silver and reactive oxygen species into solution.<sup>6–13</sup>

Two recent studies have reported that these filters can effectively remove *Escherichia coli* bacteria and turbidity from water<sup>6,7</sup> along with virus- and protozoan-sized particles.<sup>14</sup> It has

also been shown in the laboratory that the zero-valent silver nanoparticles (10–100 nm diameter) embedded in the ceramic porous media improve the removal and disinfection of *E. coli* relative to filters without silver.<sup>7</sup> This POU technology appears to be socially acceptable,<sup>6</sup> and there is evidence that the filters can improve human health in the general population<sup>15</sup> and in individuals infected with the human immunodeficiency virus (HIV).<sup>16</sup> Filter factories are gradually spreading throughout the developing world thanks to the efforts of several non-governmental agencies like Potters for Peace, FilterPure, Rural Development Partners International, and PureMadi. Based on a recent survey of global filter factories, Rayner<sup>17</sup> reports that there are 35 established filter factories in 18 countries and filter production at these factories exceeds 40 000 filters per month.

An important consideration in the design and use of ceramic filters is the application of the silver nanoparticles. Although the nanoparticles improve pathogen removal and disinfection in ceramic water filters,<sup>7</sup> the optimum dose and application method are unknown. Existing filter factories use different types of Ag-NPs, and the mass of silver applied per filter varies at

Received: January 5, 2013

Revised: March 12, 2013

Accepted: March 15, 2013

Published: March 15, 2013

least by an order of magnitude between some factories. Little is known about the retention of the Ag-NPs in the ceramic filter.

In this work, we present the first study of the transport of silver nanoparticles through ceramic porous media with a focus on investigating nanoparticle size, capping agent, solution ionic strength, and application method on the release of silver nanoparticles in the filter effluent. More importantly, we quantify silver release from filters fabricated using three different silver application methods: the conventional methods of painting onto the filter an aqueous Ag-NP suspension (paint-on method) or dipping the filter into a Ag-NP suspension (dipping method)<sup>7</sup> and a new method of adding Ag-NPs to the clay–combustible mix prior to firing (fire-in method). We hypothesize that Ag-NPs are relatively mobile in ceramic media; Ag-NPs applied by conventional methods (e.g., paint-on and dipping) result in significant Ag-NP release into solution. Furthermore, we hypothesize that application of Ag-NPs prior to firing the clay–water–sawdust mixture will result in improved Ag-NP retention relative to conventional application methods.

The experimental results and analyses herein are the first measurements published of Ag-NP transport through a ceramic porous media and the first experiments to quantify the effects of solution ionic strength, nanoparticle size, and nanoparticle capping agent on transport of the nanoparticles through ceramic media. It is also the first study to quantify the release of Ag-NPs into effluent water from ceramic media that has previously been impregnated with Ag-NPs using the fire-in method and to compare these results to Ag-NP release from ceramic media fabricated using conventional methods (paint-on and dipping). For these experiments, we have used a synthetic, moderately hard water that contains multiple monovalent and divalent inorganic ions to more closely simulate real-world conditions for ceramic filter performance.

## ■ MATERIALS AND METHODS

**Silver Nanoparticles.** Four kinds of Ag-NPs were included in this investigation. Silver proteinate (7.66% silver by mass) was obtained from Argenol Laboratories (Spain) and was used as received. This nanoparticle is supplied as a solid powder and has proteinate as a capping agent. This nanoparticle is commonly used in developing-world ceramic water filters and in other commercial applications including as an antiseptic in eyedrops and as an antimicrobial agent in plastics, textiles, cosmetics, and paints.<sup>18</sup> The proteinate capping agent is a bovine serum albumin composed of a single polypeptide chain of 583 amino acid residues.<sup>19,20</sup> Three other types were obtained from NanoComposix (San Diego, CA, USA) and belong to their NanoXact series. These particles were chosen to study the effects of nanoparticle size and capping agent on transport. They are shipped in 20 mg/L (as Ag) aqueous suspensions and were used as received; citrate is the capping agent for all three NanoComposix particles.

The mean particle diameter of each type of silver nanoparticle was measured using two methods. The first method employed dynamic light scattering (DLS) with a NiComp 380 DLS submicrometer particle sizer. DLS measurements were performed following 5-min sample sonication (Branson Ultrasonics Corp., set to 50% power) to ensure the aqueous suspension was monodisperse. The second method employed a JEOL 2000FX transmission electron microscope (TEM). Zeta potential was quantified using a Malvern Zetasizer

Nano Z. Capping agents used in nanoparticle synthesis were indicated by the manufacturers.

**Ceramic Porous Media.** Ceramic porous media were fabricated in the shape of disks as described by Oyanedel-Craver and Smith.<sup>7</sup> Briefly, 97.6 g of 200-mesh Redart pottery clay (Resco Products, Inc.) was mixed homogeneously with 122 g of 48-mesh grog (Resco Products, Inc.), and 24.4 g of flour (from a local grocery store and used as received). The dry mix (244 g) was combined with 75 mL of deionized, organic-free water (DI water) and again mixed by hand until homogeneous. The wet mixture was then divided into four equal portions with masses between 79 and 80 g. Each portion was transferred into a cylindrical plastic mold. A hand-operated press was used to compress the mixture in the mold for 1 min at 1000 psi. The pressed mixture was then removed from the mold and air-dried for two days before it was fired in a Rampmaster II electric kiln (Evenheat Kiln, Inc.). The kiln temperature was increased from room temperature to 600 °C at a rate of 150 °C/h, and then to 900 °C at a rate of 300 °C/h. The final temperature (900 °C) was held for another 3 h. The resulting cylindrical ceramic disks produced were 1.2 cm thick and 7.5 cm in diameter with a mass of  $56 \pm 1$  g.

The above-described ceramic disk fabrication method is identical to the method described previously for Redart clay by Oyanedel-Craver and Smith,<sup>7</sup> and the pore-size distribution as determined by mercury porosimetry has been previously quantified.<sup>7</sup> The  $\zeta$  potential of the ceramic porous media was determined by grinding the ceramic porous media into a powder with a mortar and pestle<sup>21</sup> and suspending the particles in aqueous MgSO<sub>4</sub> solutions of 1, 10, and 50 mM ionic strength. Each suspension was added to a folded capillary cell (DTS 1060, Malvern Instruments, Worcestershire, UK). Time-resolved hydrodynamic diameter and  $\zeta$  potential charge were monitored over 12 h at room temperature ( $24 \pm 1$  °C).<sup>18</sup>

Additional ceramic disks were fabricated using the above-described procedure but were also treated with Ag-NPs. Three different methods of Ag-NP application were studied: the “dipping” method, the “paint-on” method, and the “fire-in” method. The Ag-NPs used for these treatments were the proteinate-capped Ag-NPs from Argenol Laboratories, and the application amount resulted in either 2.76 mg or 27.6 mg of Ag per disk. The 2.76-mg Ag mass was chosen to approximately correspond to Ag application amounts recommended by Potters for Peace in the production of silver-impregnated ceramic filters. The 27.6 mg mass was chosen to represent the much-higher silver loading being used by some other filter manufacturers.

For the dipping method, each ceramic disk was submerged in a 2000 mg/L silver proteinate suspension (153 mg/L as Ag) for 5 min, air-dried for 24 h, and oven-dried to a constant weight at 80 °C (approximately 48 h). The mass of each ceramic disk before and after treatment was recorded. The difference between the two masses equaled the total weight of silver applied. Multiple disks were treated and measured in the same way. The average mass change was  $35.98 \pm 0.26$  mg ( $n = 12$ ,  $\alpha = 0.05$ ) or a mean value of 2.76 mg of Ag per disk.

Based on the dipping method results, an identical mass of silver was chosen for application using the paint-on method. For the paint-on method, a commercial paint brush was used to paint 18 mL of a 2000 mg/L aqueous suspension of silver proteinate (153 mg/L as Ag). Nine milliliters of this suspension was painted onto each side of the ceramic disk, resulting in a final mass 2.76 mg of Ag per disk.

For the fire-in method, either 143.6 mg of silver proteinate (11.04 mg as Ag) or 1.436 g of silver proteinate (110.4 mg as silver) was added to 75 mL water and sonicated. This aqueous suspension was then combined with clay, grog, and flour as described previously to construct the ceramic disks. In this manner, the silver is added *before* firing the disks, presumably providing a more homogeneous distribution of nanoparticles throughout the porous media while minimizing release of the Ag-NPs into drinking water during subsequent use of the filter. Each resulting ceramic disk fabricated using the fire-in method contained either 2.76 or 27.6 mg of Ag.

**Ag-NP Transport Experiments.** The transport of each type of Ag-NP was studied using ceramic disks fabricated without any silver addition. Each ceramic disk was placed in a flexible-wall permeameter and a high-performance liquid chromatography (HPLC) pump (Acuflow series IV) was used to inject a  $\text{MgSO}_4$  solution at a flow rate of 0.6 mL/min through the ceramic disk. This flow rate approximately corresponds to whole-filter flow rates of 2 L/h.<sup>7</sup> After 20 pore volumes of flow, the linear velocity and dispersion coefficient of the porous media was determined with a tracer test using a pulse injection of  $[\text{}^3\text{H}]\text{-H}_2\text{O}$  with subsequent analysis of the tracer breakthrough data using the one-dimensional form of the transient advection–dispersion equation. Additional details are provided in the Supporting Information.

Following the tracer test, the influent solution was changed by the addition of a 10 mg/L Ag-NP suspension for 100 min (approximately 5.8 pore volumes). The inflow solution was then changed back to the original, nanoparticle-free  $\text{MgSO}_4$  solution until the end of the experiment. Ceramic disk effluent samples were collected over time and analyzed for total silver. The  $\text{MgSO}_4$  concentration in solutions used in these experiments corresponds to ionic strengths of 1, 10, and 50 mM. These values were chosen to represent the ionic strengths of a wide range of natural fresh waters ranging from surface waters to groundwaters. These same ionic-strength levels were used to quantify the  $\zeta$  potential of the ceramic media as described earlier.

Total Ag concentrations were determined by atomic absorption spectrometry (Perkin-Elmer AAnalyst 200) following 10%  $\text{HNO}_3$  conditioning. A subset of effluent samples were analyzed for ionic silver ( $\text{Ag}^+$ ) concentrations using a calibrated silver specific-ion electrode (silver/sulfide ion selective electrode, Thermo Scientific, MA, USA). In every case, the  $\text{Ag}^+$  concentration was less than 1% of the total silver concentration, suggesting that silver ion release was relatively small over the course of each experiment. This observation is consistent with results reported by Zhang et al.<sup>22</sup> for aqueous suspensions of Ag-NPs. Therefore, it was assumed that total silver concentrations closely estimate the metallic silver ( $\text{Ag}^0$ ) concentrations in effluent samples.

The methods used for mathematical simulation of Ag-NP effluent concentrations are provided in the Supporting Information along with a summary of conditions for each experiment and the resulting parameter values (Table S1).

**Silver Release from Silver-Impregnated Ceramic Disks.** While the above-described Ag-NP transport experiments provide fundamental information about particle transport, they do not represent the retention and release of silver applied to a ceramic water filter. Therefore, experiments were performed to more closely simulate the performance of ceramic water filters under real-world conditions using the three types

of silver-impregnation methods described earlier in this section (paint-on, dipping, and fire-in). In addition, the water chemistry for the solution passed through the filter was chosen to reflect more closely a natural water with multiple monovalent and divalent inorganic ions. Previous research has shown that both the concentration and valence of inorganic ions in solution can affect nanoparticle stability.<sup>23–25</sup> The solution ionic strength and flow rate were also varied to study the effects of these variables on silver release.

The release of silver over time from disks treated using the paint-on, dipping, and fire-in methods was quantified using methods similar to those described above. Each silver-impregnated ceramic disk was placed in a flexible-wall permeameter. A synthetic, moderately hard water (96 mg/L  $\text{NaHCO}_3$ , 60 mg/L  $\text{CaSO}_4 \cdot 2\text{H}_2\text{O}$ , 60 mg/L  $\text{MgSO}_4$ , and 4 mg/L KCl) developed by the U.S. Environmental Protection Agency (and denoted as “EPA water”)<sup>26</sup> was pumped through the disk at a 0.6 mL/min flow rate for 3 h. The flow rate was then increased to 1.2 mL/min for the next 3 h. Effluent samples were collected over time and analyzed for total and ionic silver concentrations. As noted previously, ionic silver concentrations were consistently less than 1% of total silver concentrations, indicating that the silver leaving the ceramic media was in the zero-valent oxidation state. To test the impact of ionic strength on silver release from the ceramic filters, additional experiments were also performed wherein DI water was passed through the filter for the first 3 h, and then the synthetic, moderately hard EPA water was passed for the next 3 h. A first-order rate model was used to simulate effluent silver concentrations over time. The model is described in the Supporting Information and in Table S2.

## RESULTS

**Nanoparticle Characterization.** Table 1 summarizes the characteristics of each type of nanoparticle used in this

**Table 1. Summary Data for Silver Nanoparticles Used in This Investigation<sup>a</sup>**

name	DLS (nm)	TEM (nm)	$\zeta^b$ (mV)	capping agent
silver proteinate	49.0	15.8	−57.1	proteinate
NanoXact-10	13.4	8.2	−56.1	citrate
NanoXact-50	59.2	49.1	−55.6	citrate
NanoXact100	115.1	99.1	−55.4	citrate

<sup>a</sup>Data include mean particle diameter as determined by dynamic light scattering (DLS) and transmission electron microscopy (TEM),  $\zeta$  potential, and the capping agent used during synthesis. <sup>b</sup> $\zeta$  determined in deionized, organic-free water.

investigation. The NanoXact particles are marketed as having mean particle diameters of 10, 50, and 100 nm, and the measurements made in our laboratory agree well with these specifications. Mean particle diameters measured by DLS are slightly larger than the values measured using TEM. This is a typical result of these measurements, because DLS measurements include water molecules that strongly hydrate the nanoparticles and the citrate capping agent.<sup>27</sup> The DLS measurement for silver proteinate (49.0 nm) is more than three times larger than the TEM measurement (15.8 nm). This is likely caused by a macromolecular proteinate capping agent. Silver proteinate diameters measured over time by DLS reveal that the mean diameter decreases over the course of several hours, presumably as the capping agent is gradually released

into solution.<sup>18</sup> The  $\zeta$  potential values were similar for all the nanoparticles and show a negative particle surface charge.

**Ag-NP Transport Experiments.** Figure 1 and Figures S1–3, Supporting Information, show effluent concentrations of

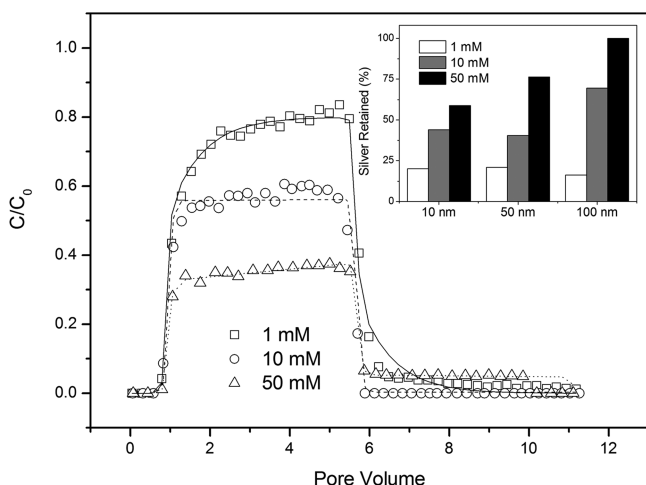


**Figure 1.** Plots of effluent total silver concentration from ceramic disks ( $C$ ) normalized to the influent total silver concentration ( $C_0$ ) as a function of pore volumes of flow for different ionic strength  $\text{MgSO}_4$  solutions (1, 10, and 50 mM). Data are for NanoXact 50 nm silver nanoparticles at a flow rate of 0.6 mL/min. Inset: Percent silver retained in the ceramic disk at each ionic strength and for all three mean nanoparticle sizes (10, 50, and 100 nm).

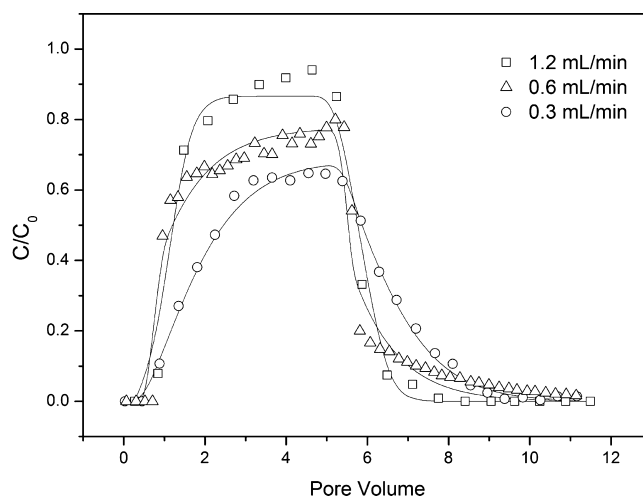
silver nanoparticles from ceramic disks normalized to the influent Ag-NP concentration as a function of pore volumes of flow. Figure 1 and Figures S1 and S3, Supporting Information, also have inset bar charts that show the percent of the inflow silver that is retained in the ceramic disk over the course of the experiment. These values were calculated by mass balance from the influent and effluent Ag-NP concentration data.

Figure 1 shows breakthrough curves for 50 nm NanoXact Ag-NPs for three different ionic strengths (1, 10, and 50 mM). As the ionic strength is increased, the effluent Ag-NP normalized concentrations plateau at decreasing values. Likewise, the percent silver retained in the ceramic disk increases with increasing ionic strength. Although the relative concentrations are only shown for the 50 nm Ag-NP, this trend is true for each type of nanoparticle as noted in the inset bar chart.

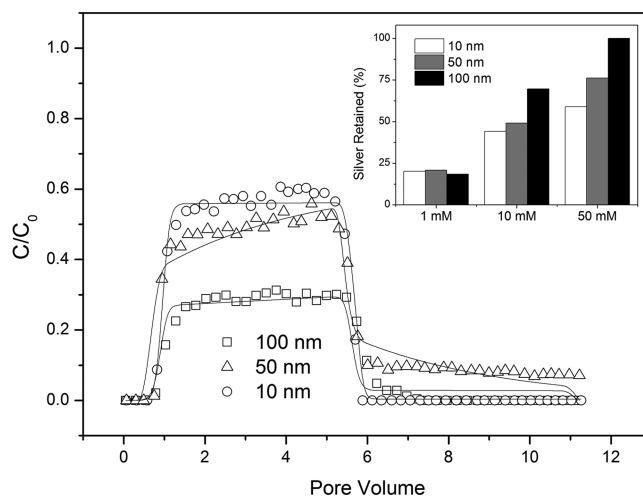
Figure S1, Supporting Information, compares the transport of Argenol silver proteinate and NanoXact-50 nanoparticles through the ceramic disks. Both show similar effluent concentration profiles. Since these particles have similar total particle sizes (including the capping agent and as measured by DLS), the results suggest that changing the capping agent from proteinate to citrate has at best only a small effect on Ag-NP transport. For each ionic strength, there is a slightly greater retention of the citrate-capped particles (inset to Figure S1, Supporting Information).

Figure 2 presents Ag-NP transport data for NanoXact-50 at flow rates of 0.2, 0.6, and 3 mL/min. By normalizing the data to pore volumes of flow, the experiments can be directly compared despite the flow rate differences. The data show that there is greater elution of Ag-NPs from the column as the flow rate is increased.

Figure 3 compares Ag-NP data for the three NanoXact particles. For 10 and 50 mM ionic strengths, the nanoparticle



**Figure 2.** Plots of effluent total silver concentration from ceramic disks ( $C$ ) normalized to the influent total silver concentration ( $C_0$ ) as a function of pore volumes of flow for three different flow rates at a  $\text{MgSO}_4$  solution ionic strength of 1 mM.



**Figure 3.** Plots of effluent total silver concentration from ceramic disks ( $C$ ) normalized to the influent total silver concentration ( $C_0$ ) as a function of pore volumes of flow for different sized NanoXact silver nanoparticles. Data are for a flow rate of 0.6 mL/min and a  $\text{MgSO}_4$  solution ionic strength of 10 mM. Inset: Percent silver retained in the ceramic disk at each ionic strength and for all three mean nanoparticle sizes.

retention in the ceramic porous media increases with Ag-NP size. For 1 mM ionic strength, the Ag-NP retention does not appear to be affected by particle size.

**Ag-NP Release Experiments.** Figures 4, 5, and 6 show results of experiments where Ag-NPs were applied to filters using the paint-on, dipping, and fire-in methods. For these cases, no Ag-NPs were present in the inflow water to the ceramic disks, but since Ag-NPs were embedded into the disk by one of the three application methods, the nanoparticles are released into the effluent water over time. Inflow solutions for these experiments used the synthetic EPA water containing both monovalent and divalent inorganic ions to better represent real-world conditions. Figure 4 shows total silver release from ceramic disks that were treated with silver by the conventional paint-on and dipping methods. For each type of disk, the flow rate was maintained at 0.6 mL/min for 180 min

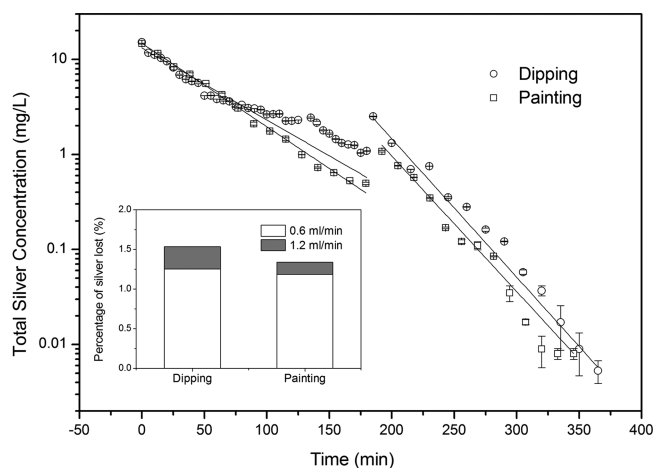


**Figure 4.** Plots of effluent total silver concentration from disks pretreated with Argenol silver nanoparticles by either painting or dipping methods. The flow rate was 0.6 mL/min from time zero to 180 min. The flow rate increased to 1.2 mL/min from 180 min to the end of the experiment. The inflow solution was a moderately hard synthetic water containing both monovalent and divalent inorganic ions. Inset: Percent of silver released from the disk for each flow rate and for each silver application method.

and then increased to 1.2 mL/min for an additional 180 min. Increasing the flow rate at 180 min causes a step increase in effluent silver. During the first 180-min period, total silver released from both types of disks is between 1.1% and 1.3% of the silver originally applied to the disk. The paint-on method appears to retain slightly more silver in the disk than the dipping method.

Figure 5 presents data similar to Figure 4 for disks manufactured using the fire-in method. Data for two different amounts of silver applied to the disks are included. The “1X” disk contains the same mass of silver as the disks prepared using the paint-on and dipping methods (2.76 mg of Ag per disk). The “10X” disks contain 27.6 mg of Ag per disk. As before, the

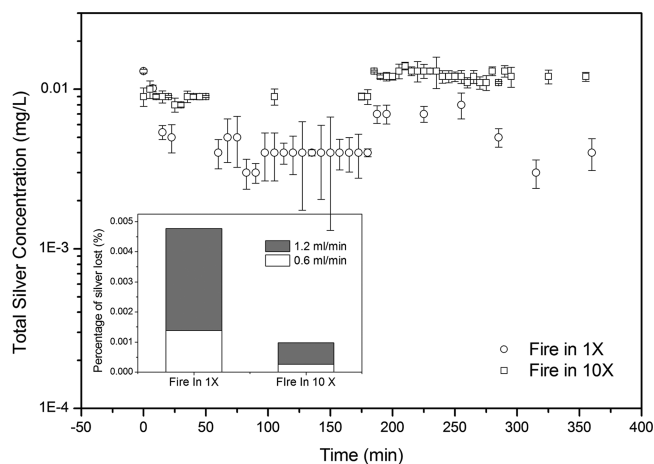


**Figure 5.** Plots of effluent total silver concentration as a function of time for disks fabricated by adding Argenol silver proteinate nanoparticles prior to firing the disk. Two different amounts of silver (varying by a factor of 10) were fired into the disks. The flow rate was 0.6 mL/min from time zero to 180 min. The flow rate increased to 1.2 mL/min from 180 min to the end of the experiment. Inset: Percent of silver released from the disk for each flow rate and for each silver application amount.

flow rate through the disks was increased from 0.6 to 1.2 mg/L after 180 min. Silver concentrations released from the 10X disk are higher than the concentrations released by the 1X disks, but when considered as a percentage of the silver applied to the disks, the 10X disks release a smaller percentage than the 1X disks. Doubling the flow rate at 180 min again caused a step increase in effluent silver concentrations followed by a return to an approximately linear decline with time. Overall, silver concentrations and percent of total silver released are significantly less than values observed for disks prepared with the paint-on and dipping methods.

Figure 6 shows how a change in solution ionic strength will affect silver release for ceramic disks prepared using the paint-

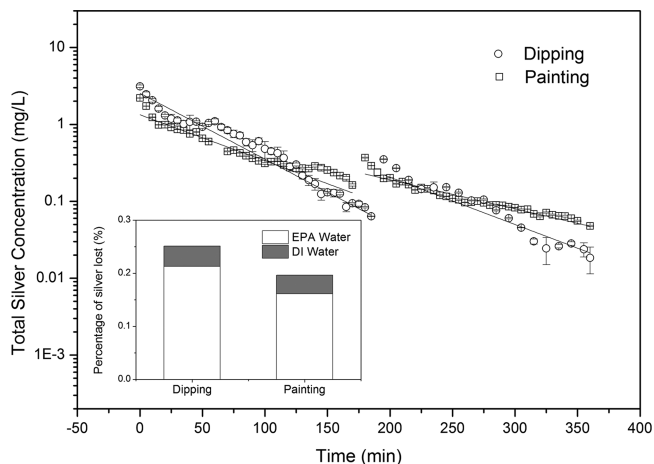


**Figure 6.** Plots of effluent total silver concentration from disks pretreated with Argenol silver nanoparticles by either painting or dipping methods. The flow rate remained constant at 0.6 mL/min for the duration of the experiment, but the ionic strength of the influent solution was changed from 10 mM (moderately hard synthetic water containing both monovalent and divalent inorganic ions) from time 0 to 180 min to 0 mM ionic strength from time 180 min until the end of the experiment. Inset: Percent of silver released from the disk for each silver application method and for each ionic strength.

on and dipping methods. The synthetic EPA water is used as inflow for the first 180 min. For the subsequent 180 min, DI water is used as inflow. The flow rate was maintained at 0.6 mL/min for the duration of this experiment. At 180 min, there is a step increase in effluent silver for both paint-on and dipping disks. Silver concentrations then decrease approximately linearly over time at a slope that is equal to or slightly greater than the slope from the first 180-min period.

## DISCUSSION

**Ag-NP Transport through Ceramic Porous Media.** Ag-NPs are relatively mobile through the ceramic porous media under certain conditions. The extent of mobility depends on both the nanoparticle properties and the water chemistry. Table S1, Supporting Information, and the bar charts that are inset in Figures 1 and 3 show that the percent of silver applied that exits the ceramic disks can be as high as 87%. This is significant given that ceramic water filters are generally believed to retain silver nanoparticles and remove turbidity from inflow water. Ag-NP mobility is closely related to solution ionic strength and, to a lesser extent, nanoparticle size.

Throughout all the experiments in this study, increased ionic strength correlates with decreases in Ag-NP mobility (Figures 1

and 6). This behavior is likely caused by two mechanisms. First, increasing ionic strength can compress the diffuse double layer surrounding the Ag-NPs. This causes increased particle–particle interaction resulting in aggregation and increased physical filtration (straining) of the nanoparticle clusters.<sup>22,28–31</sup> Second, the reduction in the diffuse double layer surrounding the Ag-NPs likely reduces the repulsive forces between the nanoparticle and the surface of the ceramic porous media.<sup>30,31</sup> For deposition of Ag-NPs onto the ceramic surface to occur, the primary energy barrier (according to DLVO theory) must be overcome. For negatively charged particle deposition onto a like-charged surface, the primary energy barrier is reduced with increasing ionic strength. Therefore, the increased retention of the Ag-NPs with increasing ionic strength may be caused by increased attraction between the nanoparticle and the ceramic porous media surface.

Based on the  $\zeta$  potential measurements (Table 1) for each type of Ag-NP used in this investigation and the  $\zeta$  potential measured for the ceramic media at ionic strengths of 1, 10, and 50 mM, interaction energies between the Ag-NPs and the ceramic collector surfaces can be quantified using the Derjaguin–Landau–Verwey–Overbeek (DLVO) theory. Details of the calculation method along with plots of interaction energies as a function of separation distance for each nanoparticle and ionic strength are presented in the Supporting Information (Figures S2–S5). Peak interaction energies for each ionic strength and Ag-NP combination are shown in Table 2. As expected, interaction energies are significantly reduced as

**Table 2. Peak Interaction Energies between Four Types of Silver Nanoparticles and the Ceramic Porous Medium at Three Ionic Strengths**

interaction energy ( $k_B T$ )	ionic strength (mM)		
	1	10	50
silver proteinate	26.53	6.82	0.75
NanoXact-10	4.38	0.98	0.12
NanoXact-50	24.60	6.32	0.70
NanoXact-100	51.56	13.25	1.47

solution ionic strength is increased. These analyses further support the observed reduced transport of Ag-NPs through the ceramic porous media with increase ionic strength shown in Figures 1 and 6. Although this is the first study to present results of Ag-NP transport through a ceramic porous medium, Ren and Smith<sup>18</sup> have recently shown that Ag-NP transport through water-saturated sand porous media also decreases with increasing ionic strength. Although they reported some particle aggregation, they identified increased deposition of nanoparticles on the sand surfaces as the main reason for this behavior. Likewise, several other recent publications have shown that ferrihydrite and fullerene nanoparticle stability and transport is reduced in sand and soil porous media as ionic strength is increased.<sup>32,33</sup>

These observations have a practical implication. Ceramic filters impregnated with Ag-NPs may release more silver if the source water is a surface water instead of a groundwater. Groundwaters typically have higher ionic strengths than surface waters. For a given amount of applied silver, the silver's longevity in the filter may therefore be less for surface water compared with groundwater. Additionally, release of silver into the filter effluent and consumption by the user will likely be greater for surface water than groundwater.

Ag-NP size appears to have some effect on transport, but to less extent than ionic strength. The inset bar chart in Figure 3 compares nanoparticle retention in the ceramic porous media for the 10, 50, and 100 nm Ag-NPs for each ionic strength. For 1 and 10 mM ionic strengths, there does not appear to be any discernible effect of particle size on Ag-NP retention in the porous media. However, for 50 mM ionic strength, Ag-NP retention increases with particle size.

The effect of particle size on Ag-NP transport may be influenced by multiple factors.<sup>34</sup> Consideration of physical filtration alone would suggest that larger particles will be less mobile than smaller particles. Consideration of our DLVO theory energy barriers show that small particles will be retained more than large particles because the peak interaction energy decreases with decreasing particle size (Table 2). The  $\zeta$  potential may also vary with particle size, although for our Ag-NPs there was negligible change in  $\zeta$  potential from our 10–100 nm particles (Table 1). A recent study by Wang et al.<sup>34</sup> studied the effects of silica nanoparticle size on retention in sand porous media. They found that the relative retention of 8 nm particles was slightly greater than for 52 nm particles. They attributed this result to larger deposition rate coefficient ( $k_d$ ) values for the 8 nm particles relative to the 52 nm particles. For the largest Ag-NP studied (100 nm), physical filtration may have been significantly more important than particle–collector interaction, and a positive correlation between particle size and particle retention was observed.

**Ag-NP Release from Silver-Impregnated Ceramic Porous Media.** Perhaps the most important result of this work pertains to the release of silver nanoparticles that have been previously applied to the ceramic porous media by the paint-on, dipping, or fire-in methods. Figures 4 and 5 show that while there may not be much difference between the paint-on and dipping methods of silver application, the fire-in method appears to significantly improve nanoparticle retention in the ceramic porous media. In the first 180 min of use, ceramic disks treated with silver using the paint-on and dipping methods release slightly more than 1% of the original amount of silver applied and effluent concentrations range between 1 and 10 mg/L. These values are more than 10 times greater than the drinking-water standard for silver of 0.1 mg/L. By contrast, slightly greater than 0.001% of silver was released from ceramic disks with silver fired-in over the first 180 min, approximately 1000 times less than the paint-on and dipping methods. Furthermore, the effluent silver concentrations never exceed 0.02 mg/L, which is about 5 times lower than the drinking water standard for silver. Even when the amount of silver applied to the disk is increased by a factor of 10 (e.g., fire-in 10X, Figure 5), the effluent concentration never exceeds 0.02 mg/L. These results suggest that for silver retention in the filter, the fire-in method will produce a significant improvement in performance. During the firing process, the Ag-NPs presumably concentrate in the smallest-diameter pores (as water likely evaporates from the largest pores first) or they may simply exist in pores disconnected with the flow field. Concentration of the silver in the smallest pores likely minimizes their mobilization in the pore water. For the conditions of our work, the maximum firing temperature (900 °C) does not exceed the melting point of silver (961 °C).

We should note that although the results in Figure 4 show silver levels greater than the drinking water standard for silver, concentrations are declining exponentially with time. Therefore, silver levels in the effluent water likely will fall below

drinking water standards within a few hours of use. This result is consistent with silver levels reported by Oyanedel-Craver and Smith<sup>7</sup> in laboratory studies and by field data in Guatemala reported by Kallman et al.<sup>6</sup> Nevertheless, the higher rate of silver release likely renders the filter less effective over time compared with filters fabricated with the fire-in method.

The paint-on method appears to retain slightly more silver than the dipping method (Figure 4). This may be caused by capillary effects. For the dipping method, the aqueous Ag-NP suspension applied to the ceramic porous media is always at a pressure greater than atmospheric, and water and nanoparticles will fill both large and small pores. By contrast, for the paint-on method, the aqueous Ag-NP suspension is drawn into the ceramic disk by capillary action, with the smallest pores filling first. Therefore, Ag-NPs are preferentially deposited in the smaller pores relative to larger pores. This likely results in a small increase in retention of the Ag-NPs because it is more difficult to dislodge Ag-NPs from small pore spaces relative to larger pore spaces.

Changes in flow rate and solution ionic strength also appear to influence silver release (Figures 4, 5, and 6). Increasing the interstitial water velocity likely dislodges Ag-NPs that were otherwise immobilized in the ceramic porous media. This result has also been observed for the transport of ferrihydrite nanoparticles in a quartz sand porous medium.<sup>32</sup> Likewise, reduction in solution ionic strength reduces particle–particle and particle–surface attractive forces and likely increases Ag-NP mobility. For the results shown in Figures 4–6, the inflow solution was a moderately hard synthetic water containing both monovalent and divalent inorganic ions. It should be noted that natural waters also typically contain milligram per liter levels of dissolved organic matter (DOM). Prior research has indicated that DOM can increase stability of titanium dioxide nanoparticles with respect to silica surfaces by steric repulsion and repulsive electrostatics even under relatively high ionic strength conditions.<sup>35</sup> Therefore, it is possible that silver nanoparticle mobility could be increased in the presence of DOM.

For the 1X and 10X fire-in methods, we can make very rough estimates of the time until the silver in the filter is depleted. For a flow rate of 0.6 mL/min, the effluent silver concentration maintains a relatively steady value of 0.004 mg/L for the 1X fire-in method (Figure 5). These ceramic disks contain 2.76 mg of Ag. Therefore, over a 1-h flow period, the mass fraction of silver removed from the disk is  $5.174 \times 10^{-5}$ , and it would take about 19 300 h of flow to deplete all the silver assuming a constant silver release rate and that all the silver can be released from the ceramic porous medium. The 0.6 mL/min flow rate of the ceramic disk corresponds approximately to a 1.5 L/h flow rate for a whole-pot filter.<sup>7</sup> If we assume water is being filtered 24 h per day, the silver will be depleted in 805 days or 2.2 years. A similar calculation for the 10X fire-in method (with a relatively constant effluent silver concentration of 0.009 mg/L and a silver mass in the disk of 27.6 mg) results in a predicted silver depletion time of 3550 days or 9.7 years. Of course in practice, it is unlikely that water will be filtered 24 h per day at a 1.5 L/h flow rate.<sup>36</sup> It is more difficult to predict the depletion of silver for the paint-on and dipping methods, because the effluent silver concentration generally decreases with time. However, over the course of these experiments, the paint-on and dipping methods release about 1000 times more silver than the fire-in method.

Although the fire-in method appears to be an improved way of applying Ag-NPs to ceramic water filters due to its increased

retention of the silver, no data has yet been presented to show that this method results in equal or better disinfection of pathogens entering the filter. The fire-in method likely results in a more homogeneous distribution of the silver throughout the porous media (which should improve pathogen disinfection); it is also possible that some of the silver resides in pores that are disconnected from continuous flow paths and do not contribute to disinfection. For fabrication of whole-pot filters, the conventional dipping and paint-on methods are performed only for filters that have been fired and tested for adequate flow rates. For the fire-in method, silver is applied prior to firing during the clay–sawdust–water mixing process. Therefore, the silver applied to filters that break during firing or that do not pass flow-test requirements is essentially wasted. Successful filter factories typically have 90% or more of their filters pass flow-rate quality assurance tests, so the fire-in method would increase silver material costs by about 10% relative to the paint-on or dipping methods. On the other hand, the fire-in method is less labor intensive than the paint-on or dipping methods and would thereby reduce production costs.

## ■ ASSOCIATED CONTENT

### 📄 Supporting Information

Formulation of the Ag-NP transport model, the first-order rate model to simulate silver release from ceramic disks fabricated using silver, fitted model rate parameters, and figures and methods for the determination of interaction energies between Ag-NPs and the ceramic collector surface. This material is available free of charge via the Internet at <http://pubs.acs.org>.

## ■ AUTHOR INFORMATION

### Notes

The authors declare no competing financial interest.

## ■ ACKNOWLEDGMENTS

This research was supported by the U.S. National Science Foundation (Grant CBET 0854047) and the Environmental Research and Education Foundation (EREF).

## ■ REFERENCES

- (1) Clasen, T.; Roberts, I.; Rabie, T.; Schmidt, W.; Cairncross, S. Interventions to improve water quality for preventing diarrhoea. *Cochrane Libr.* **2006**, *3*, 1–99.
- (2) Clasen, T.; Nadakatti, S.; Menon, S. Microbiological performance of a water treatment unit designed for household use in developing countries. *Trop. Med. Int. Health* **2006**, *11* (9), 1399–1405.
- (3) Ceramics Manufacturing Working Group *Best practice recommendations for local manufacturing of ceramic filters for water treatment*; Seattle, 2010.
- (4) Lantagne, D. S. *Investigation of the Potters for Peace colloidal silver impregnated ceramic filter*; USAID: Washington, DC, December 21, 2001; p 79.
- (5) Hunter, P. R. Household water treatment in developing countries: Comparing different intervention types using meta-regression. *Environ. Sci. Technol.* **2009**, *43* (23), 8991–8997.
- (6) Kallman, E.; Oyanedel-Craver, V.; Smith, J. A. Ceramic filters impregnated with silver nanoparticles for point-of-use water treatment in rural Guatemala. *J. Environ. Eng.* **2011**, *137* (6), 407–415.
- (7) Oyanedel-Craver, V.; Smith, J. A. Sustainable colloidal-silver-impregnated ceramic filter for point-of-use water treatment. *Environ. Sci. Technol.* **2008**, *42* (3), 927–933.
- (8) Choi, O.; Hu, Z. Role of reactive oxygen species in determining nitrification inhibition by metallic/oxide nanoparticles. *J. Environ. Eng.* **2009**, *135* (12), 1365–1370.

- (9) Choi, O. K.; Hu, Z. Q. Nitrification inhibition by silver nanoparticles. *Water Sci. Technol.* **2009**, *59*, 1699–1702.
- (10) Choi, O.; Hu, Z. Size dependent and reactive oxygen species related nanosilver toxicity to nitrifying bacteria. *Environ. Sci. Technol.* **2008**, *42*, 4583–4588.
- (11) Marones, J.; Elechiguerra, J.; Camacho, A.; Holt, K.; Kouri, J.; Ramirez, J.; Yacaman, M. The bactericidal effect of Ag nanoparticles. *Nanotechnology* **2005**, *16*, 2346–2353.
- (12) Lok, C.-N.; Ho, C.-M.; Chen, R.; He, Q.-Y.; Yu, W.-Y.; Sun, H.; Tam, P. K.-H.; Chiu, J.-F.; Che, C.-M. Silver nanoparticles: Partial oxidation and antibacterial activities. *JBIC, J. Biol. Inorg. Chem.* **2007**, *12*, 527–534.
- (13) Dankovich, T. A.; Gray, D. G. Bactericidal paper impregnated with silver nanoparticles for point-of-use water treatment. *Environ. Sci. Technol.* **2011**, *45* (5), 1992–1998.
- (14) Bielefeldt, A. R.; Kowalski, K.; Schilling, C.; Schreier, S.; Kohler, A.; Summers, R. S. Removal of virus to protozoan sized particles in point-of-use ceramic water filters. *Water Res.* **2010**, *44* (5), 1482–1488.
- (15) Brown, J.; Sobsey, M. D.; Loomis, D. Local drinking water filters reduce diarrheal disease in Cambodia: A randomized, controlled trial of the ceramic water purifier. *Am. J. Trop. Med. Hyg.* **2008**, *79* (3), 394–400.
- (16) Abebe, L. S.; Narkiewicz, S.; Singo, A.; Brant, J.; Oyanedel-Craver, V.; Amidou, S.; Conaway, M.; Smith, J. A.; Dillingham, R. Ceramic water filters impregnated with silver nanoparticles as a point-of-use water-treatment intervention for HIV-positive individuals in Limpopo Province, South Africa: A pilot study of technological performance and human health benefits. *J. Trop. Med. Hyg.* **2013**, submitted for publication.
- (17) Rayner, J. Current Practices in Manufacturing of Ceramic Pot Filters for Water Treatment. Master of Science, Loughborough University, 2009.
- (18) Ren, D.; Smith, J. A. Proteinate-capped silver nanoparticle transport in water-saturated sand. *J. Environ. Eng.* **2013**, DOI: 10.1061/(ASCE)EE.1943-7870.0000684.
- (19) Elechiguerra, J. L.; Burt, J. L.; Morones, J. R.; Camacho-Bragado, A.; Gao, X.; Lara, H. H.; Yacaman, M. J. Interaction of silver nanoparticles with HIV-1. *J. Nanobiotechnol.* **2005**, *3* (6), 1–10.
- (20) Peters, T. J. *All About Albumin: Biochemistry, Genetics, and Medical Applications*; Academic Press: San Diego, CA, 1996.
- (21) Bradford, S. A.; Kim, H. Implications of cation exchange on clay release and colloid-facilitated transport in porous media. *J. Environ. Qual.* **2010**, *39*, 2040–2046.
- (22) Zhang, H.; Smith, J. A.; Oyanedel-Craver, V. The effect of natural water conditions on the anti-bacterial performance and stability of silver nanoparticles capped with different polymers. *Water Res.* **2012**, *46*, 691–699.
- (23) Chen, K. L.; Mylon, S. E.; Elimelech, M. Aggregation kinetics of alginate-coated hematite nanoparticles in monovalent and divalent electrolytes. *Environ. Sci. Technol.* **2006**, *40*, 1516–1523.
- (24) Chen, K. L.; Elimelech, M. Interaction of fullerene (C60) nanoparticles with humic acid and alginate coated silica surfaces: Measurements, mechanisms, and environmental implications. *Environ. Sci. Technol.* **2008**, *42*, 7607–7614.
- (25) Thio, B. J. R.; Lee, J.-H.; Meredith, J. C.; Keller, A. A. Measuring the influence of solution chemistry on the adhesion of Au nanoparticles to mica using colloid probe atomic force microscopy. *Langmuir* **2010**, *26* (17), 13995–14003.
- (26) U.S. Environmental Protection Agency Dilution Water. [http://water.epa.gov/scitech/methods/cwa/wet/upload/2007\\_07\\_10\\_methods\\_wet\\_disk2\\_atx7-10.pdf](http://water.epa.gov/scitech/methods/cwa/wet/upload/2007_07_10_methods_wet_disk2_atx7-10.pdf).
- (27) MacCusprie, R. I.; Rogers, K.; Patra, M.; Suo, Z.; Allen, A. J.; Martin, M. N.; Hackley, V. A. Challenges for physical characterization of silver nanoparticles under pristine and environmentally relevant conditions. *J. Environ. Monit.* **2011**, *13* (5), 1212–1226.
- (28) Zhang, H.; Oyanedel-Craver, V. Evaluation of the disinfectant performance of silver nanoparticles in different water chemistry conditions. *J. Environ. Eng.* **2012**, *138* (1), 58–66.
- (29) Jaisi, D. P.; Elimelech, M. Single-walled carbon nanotubes exhibit limited transport in soil columns. *Environ. Sci. Technol.* **2009**, *43* (24), 9161–9166.
- (30) Elimelech, M.; Gregory, J.; Jia, X.; Williams, R. A. *Particle deposition and aggregation: Measurement, modeling, and simulation*. Butterworth-Heinemann: Oxford, U.K., 1995; p 441.
- (31) Tian, Y.; Gao, B.; Silvera-Batista, C.; Ziegler, K. J. Transport of engineered nanoparticles in saturated porous media. *J. Nanopart. Res.* **2010**, *12* (7), 2371–2380.
- (32) Tosco, T.; Bosch, J.; Meckenstock, R. U.; Sethi, R. Transport of ferrihydrite nanoparticles in saturated sand porous media: Role of ionic strength and flow rate. *Environ. Sci. Technol.* **2012**, *46* (7), 4008–4015.
- (33) Zhang, L.; Hou, L.; Wang, L.; Kan, A. T.; Chen, W.; Tomson, M. B. Transport of fullerene nanoparticles (nC60) in saturated sand and sandy soil: Controlling factors and modeling. *Environ. Sci. Technol.* **2012**, *46*, 7230–7238.
- (34) Wang, C.; Bobba, A. D.; Attinti, R.; Shen, C.; Lazouskaya, V.; Wang, L.-P.; Jin, Y. Retention and transport of silica nanoparticles in saturated porous media: Effect of concentration and particle size. *Environ. Sci. Technol.* **2012**, *46* (13), 7151–7158.
- (35) Thio, B. J. R.; Zhou, D.; Keller, A. A. Influence of natural organic matter on the aggregation and deposition of titanium dioxide nanoparticles. *J. Hazard. Mater.* **2011**, *189* (1–2), 556–563.
- (36) Schweitzer, R. W.; Cunningham, J. A.; Mihelcic, J. R. Hydraulic modeling of clay ceramic water filters for point-of-use water treatment. *Environ. Sci. Technol.* **2013**, *47*, 429–435.